

DIRECT NUMERICAL SIMULATION OF THE FLOW OVER A SPHERICAL BUBBLE IN A TURBULENT PIPE FLOW

L. Jofre^{1,*}, N. Balcázar^{1,*}, O. Lehmkuhl^{1,2}, R. Borrell² and J. Castro¹

¹Heat and Mass Transfer Technological Center, Technical University of Catalonia,
C/ Colom 11, 08222 Terrassa, Spain. E-mail: cttc@cttc.upc.edu

²Termo Fluids S.L., Av. Jacquard 97 E, 08222 Terrassa, Spain.
E-mail: termofluids@termofluids.com

Key words: Bubble, DNS, Multiphase, Turbulence, Pipe Flow.

Abstract. This work aims at investigating, by means of a direct numerical simulation, the flow over a clean spherical bubble fixed on the axis of a turbulent pipe flow. The simulation is performed by means of a parallel unstructured symmetry-preserving formulation on a mesh of 5.4M cells. The main features of the turbulent flow are described by analyzing the time-averaged data collected over a significant period of time. The numerical results conclude that the bubble generates a wake, similarly to the case of a solid sphere, however, it differs in the fact that the fluid slips through the surface of the bubble instead of stopping, thus, no boundary layer is created. Moreover, due to viscosity, a transfer of momentum from the fluid surrounding the bubble to the fluid inside of it is produced. This transfer of momentum generates a turbulent toroidal vortex inside the bubble. In consequence, two short recirculation zones are found at the extremes of the bubble's diameter, while in between, the axial velocity inverts its sign.

1 INTRODUCTION

The flow over a high-Reynolds-number clean spherical bubble fixed on the axis of a turbulent pipe flow falls into the classification of bubbly flow, which differs in three important aspects from bluff body flows. First, when the liquid is pure enough, it has the possibility to slip along the surface of the bubbles, in contrast to the flow over rigid bodies where the no-slip condition prevails. Second, due to the very small relative density of the bubbles compared to that of the liquid, almost all the inertia is contained in the liquid, making inertia induced hydrodynamic forces particularly important in the prediction of bubble motion. Third, the shape of the bubbles may change with the local forces, adding new degrees of freedom to an already complex problem. All these general differences together with other particular characteristics are extensively described in the work by Magnaudet et al. [1], which analyzes the motion of high-Reynolds-number bubbles in

inhomogeneous flows. Moreover, other studies of the flow around clean spherical bubbles, written by the same authors, may be found in the scientific literature [2, 3, 4, 5].

The objective of this work is to solve and analyze the flow over a spherical bubble fixed at the center of a turbulent pipe flow. The computations have been performed using a parallel unstructured conservative formulation adequate for solving turbulent flows on complex geometries. The numerical details of the discrete model utilized are given in Sec. 2, while Sec. 3 describes the statement of the problem and the computational domain used. Next, the numerical results and their corresponding analysis are exposed in Sec. 4. Finally, conclusions are drawn at the end of the work.

2 MATHEMATICAL AND NUMERICAL MODEL

The interface between two or more immiscible fluids constitutes a material surface whose motion is described by

$$\frac{d\mathbf{x}_\Gamma}{dt} = \mathbf{u}(\mathbf{x}_\Gamma, t), \quad (1)$$

where subscript Γ refers to a point on the interface between fluids. One option to solve this equation is to chase the different fluids as they move by embedding them into a static grid with the help of scalar values. This approach is commonly named interface-capturing, in which the Volume-of-Fluid (VOF) [7] and Level-Set (LS) [8] are the two most important methods. These methods define a fluid-volume fraction, C_k , as the portion of volume filled with fluid k , expressed as

$$C_k = \frac{1}{V_\Omega} \int_\Omega H(\mathbf{x} - \mathbf{x}_\Gamma) d\mathbf{x}, \quad (2)$$

where H is the Heaviside function, providing, for each fluid k , a continuity equation for the fluid-volume fraction, written in discrete matrix operators as

$$\mathbf{\Omega} \frac{dC_k}{dt} + \mathbf{C}(\mathbf{u})C_k = 0, \quad (3)$$

where the diagonal matrix $\mathbf{\Omega}$ describes the volume of cells and the matrix $\mathbf{C}(\mathbf{u})$ represents the convective operator.

On the other hand, multiphase flows of immiscible fluids are governed by the mass and Navier-Stokes equations in the variable-density incompressibility limit, which may be discretized on a general mesh scheme, using discrete matrix operators, as

$$\mathbf{M}\mathbf{u} = \mathbf{0}, \quad (4)$$

$$\mathbf{\Omega} \frac{d(\rho\mathbf{u})}{dt} + \mathbf{C}(\rho\mathbf{u})\mathbf{u} + \mathbf{G}\mathbf{p} + \mathbf{D}(\mu)\mathbf{u} + \mathbf{\Omega}\mathbf{S} = \mathbf{0}, \quad (5)$$

where \mathbf{u} , \mathbf{p} and \mathbf{S} are the vectors of velocities, pressures and source terms, e.g., gravitational acceleration, $\rho\mathbf{g}$, and surface tension, \mathbf{T}_σ , and matrices $\mathbf{C}(\rho\mathbf{u})$ and $\mathbf{D}(\mu)$ are the

convective and diffusive operators, while matrices \mathbf{G} and \mathbf{M} represent the gradient and divergence operators. Additionally, density, ρ , and dynamic viscosity, μ , are interpolated from the properties of each fluid k by means of the fluid-volume fraction values as

$$\rho = \sum_k C_k \rho_k \quad \text{and} \quad \mu = \sum_k C_k \mu_k. \quad (6)$$

The fluid-volume fraction continuity equation, Eq. 3, has been discretized by means of a VOF method [9], while the mass, Eq. 4, and Navier-Stokes, Eq. 5, equations have been discretized on a collocated mesh scheme [10]. In particular, the collocated discretization utilized conserves mass and momentum exactly, while minimizes the error in the conservation of kinetic energy. This is an important property when solving turbulent flows, since kinetic energy is convected from the main flow into the large eddies, and from them into the next smaller ones, and so on until it is dissipated by the smallest eddies found. Hence, if no external sources are present, the rate of change of total energy is just determined by dissipation. Thus, discretization strategies with excessive numerical dissipation can alter the physics of a problem in a very important proportion.

In detail, the collocated scheme used in this work solves the velocity-pressure coupling of the momentum equation, Eq. 5, by means of a classical fractional step projection method, the convective and diffusive terms are explicitly evaluated by a second-order Adams-Bashforth time integration scheme, while for the pressure gradient and source terms, an implicit first-order scheme has been used. As studied in a previous work [10], when the fractional step method on a collocated arrangement is used, there are two sources of errors in the kinetic energy conservation: (1) due to the interpolation schemes and (2) due to the difference in pressure gradient evaluation necessary to exactly conserve mass. The first one can be eliminated through the use of symmetry-preserving schemes [11], while the second one has been shown to be proportional to the density ratio and scaled by the mesh size and time step as $\mathcal{O}(\Delta h^2, \Delta t^m)$. Hence, in the case of direct numerical simulations (DNS), this error is highly minimized and usually imperceptible for the physics of the problems.

3 STATEMENT OF THE PROBLEM

The problem consists of a spherical bubble (*abbrv. bl*), with diameter d and density ρ_{bl} , placed fixed at $y = 0$ on the y -axis of a circular pipe, having diameter D and length L , that contains a fluid (*abbrv. fl*) of density $\rho_{fl} = 10\rho_{bl}$. The Cartesian coordinate system attached to the bubble is (x, y, z) . The physics of the problem depends on the bulk and bubble Reynolds numbers. The first one, bulk Reynolds number, is defined as $Re = \rho_{fl} u_{bk} D / \mu_{fl}$, where u_{bk} refers to the bulk velocity. The second one, bubble Reynolds number, is expressed as $Re_{bl} = \rho_{bl} u_{bl} d / \mu_{bl}$, being u_{bl} the time-averaged y -velocity of the flow at the center of the bubble in absolute value. In particular, this test chooses ρ_{bl} , Re , Re_{bl} and u_{bk} as 1, 6000, 500 and 1, respectively, selected in this way so that the size of the bubble is comparable to the Taylor microscale of the flow and is about ten times

the Kolmogorov microscale. The relation between pipe length and diameter is $L = 5D$ and the bubble's diameter is chosen as $L = 78d$. In this way, the pipe is long enough to include even the largest-scale structures, and the velocity defect in the bubble's wake is significantly decreased before re-entering through the inlet boundary due to the periodic condition.

The bubble is assumed to be clean, i.e., free of any surfactant or contaminant, and the surface tension to be high enough for its shape to remain spherical. Under these assumptions, the normal velocity and tangential stress are zero at the bubble surface, written as

$$\left. \begin{aligned} \mathbf{u} \cdot \mathbf{n}_\Gamma &= 0 \\ \mathbf{n}_\Gamma \times (\boldsymbol{\tau} \cdot \mathbf{n}_\Gamma) &= \mathbf{0} \end{aligned} \right\} \text{ for } r = d/2, \quad (7)$$

where \mathbf{n}_Γ is the unit vector normal to the surface of the bubble and $\boldsymbol{\tau} = \mu(\nabla \mathbf{u} + \nabla^T \mathbf{u})$ refers to the viscous part of the stress tensor. Accordingly, a no-slip boundary condition is imposed at the pipe wall, while a periodic condition connects the inlet and outlet of the pipe. In addition, the flow in the pipe is driven by forcing a pressure difference, ΔP , between the outlet and the inlet. In detail, the averaged momentum balance in the pipe implies that ΔP is directly related to the average shear stress at the pipe wall, $\rho_{fl} u_{\tau_0}^2$ — neglecting the average force acting on the bubble, since it turns out to be small compared to that of the average wall shear stress. In this way, ΔP may be defined as

$$\frac{\Delta P}{L} = \frac{-4\rho_{fl} u_{\tau_0}^2}{D}, \quad (8)$$

where u_{τ_0} is the wall shear velocity, which, in the case that $Re > 4000$, the Blasius empirical correlation evaluates it as

$$u_{\tau_0} = u_{bk} \left(\frac{0.3164 Re^{-1/4}}{8} \right)^{1/2}. \quad (9)$$

The computational domain is discretized by rotating 360° a 2-D grid around the y -axis, as exemplified in Fig. 1. In particular, the grid spacing must satisfy requirements for the correct resolution of both the pipe and bubble's boundary layer and bubble's wake. Hence, the mesh is made up of 5.4M cells, resulting from rotating 128 times the 2-D grid discretized by means of 128 points (concentrated on the pipe wall and the bubble) in the radial direction and 330 points (accumulated at the bubble) in the axial direction. In detail, the 2-D mesh contains the first radial point near the pipe wall at $r^+ = 0.94$ — similarly to the grid spacing used for the DNS of the turbulent pipe flow at $Re = 5300$ by Eggels et al. [12]. Furthermore, the mesh is generated such that at least three cells lie within the bubble's boundary layer — an estimate of the thickness is $\delta/d \sim Re_{bl}^{-1/2}$ [13] —, which, according to Legendre and Magnaudet [3], is a necessary condition in order to properly solve all the scales in the vicinity of the bubble.

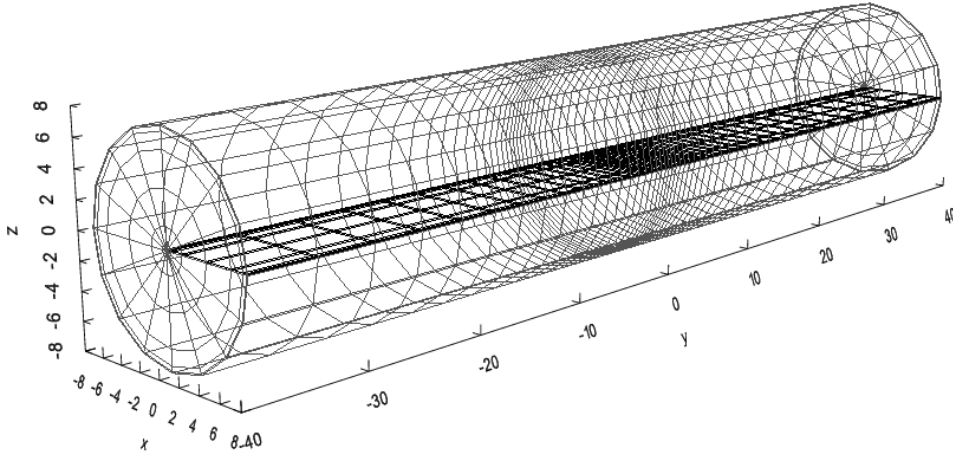


Figure 1: Example of a 3-D mesh generated by rotating a 2-D grid around the y -axis. This mesh is a coarse version of the one used for the calculations, however, correctly exemplifies the grid refinement near the pipe wall and bubble surface.

4 NUMERICAL RESULTS

4.1 Turbulent pipe flow at Reynolds number 5300

Prior to simulating the flow over the spherical bubble, the solution of the turbulent pipe flow at $Re = 5300$ without the bubble is analyzed. This initial test, aside of being a method to check the code without interfaces, will generate a fully developed turbulent flow useful to start the simulation of the bubble. The computations are performed in the same domain, which in this case is discretized as in the DNS by Eggels et al. [12]: $96 \times 128 \times 256$ gridpoints equally spaced in the radial, rotational and axial directions, respectively. This mesh configuration produces a rotational coupling of the discrete Poisson's pressure equation, resulting in circulant submatrices that are diagonalizable in a Fourier space. This allows us to solve the Poisson's pressure equation by means of a Fast Fourier Transform (FFT) method. The algorithm used is a combination of a direct Schur complement based decomposition (DSD) and a Fourier diagonalization. The latter decomposes the original system into a set of mutually independent 2-D systems, which are solved by means of the DSD algorithm. For more details the reader is referred to Borrell et al. [14].

The problem is initiated with a random sinusoidal velocity field at dimensionless time $t^* = u_{\tau_0} t / D = 0$, reducing in this way the required time to reach the statistically steady state. In fact, at $t^* = 2.0$ the average turbulent flow can be considered steady, thus, from this point the collection of average data is initialized until $t^* = 4.0$. The results are found to be in good agreement with the DNS results reported by Eggels et al. [12]: the profile of the axial mean velocity scaled in wall coordinates, u_y^+ , as function of the wall distance, r^+ , is shown in Fig. 2, while the root-mean-square (rms) values of the fluctuating velocities, u_{rms} , normalized by the wall shear velocity, u_{τ_0} , are shown in Fig. 3 using wall coordinates.

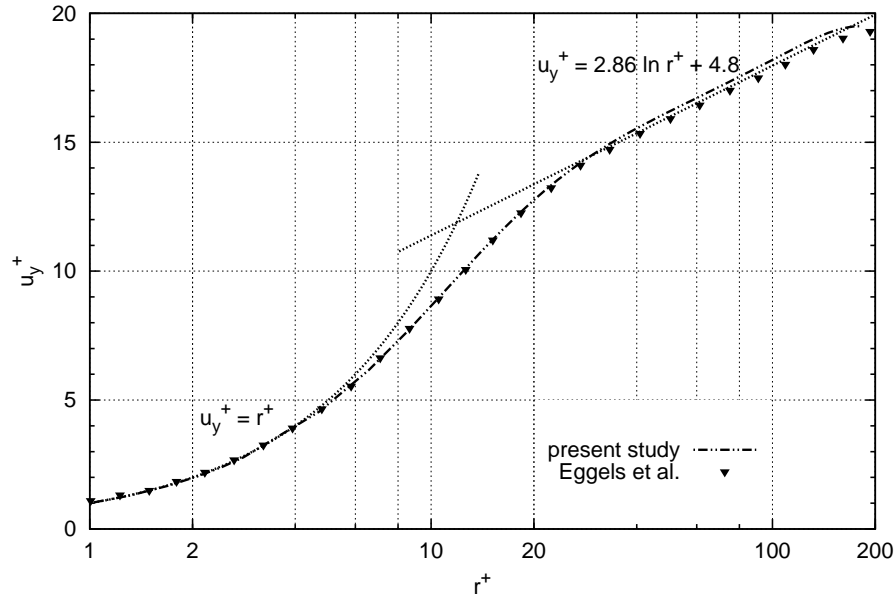


Figure 2: Axial mean velocity scaled in wall coordinates, u_y^+ , as function of the wall distance, r^+ .

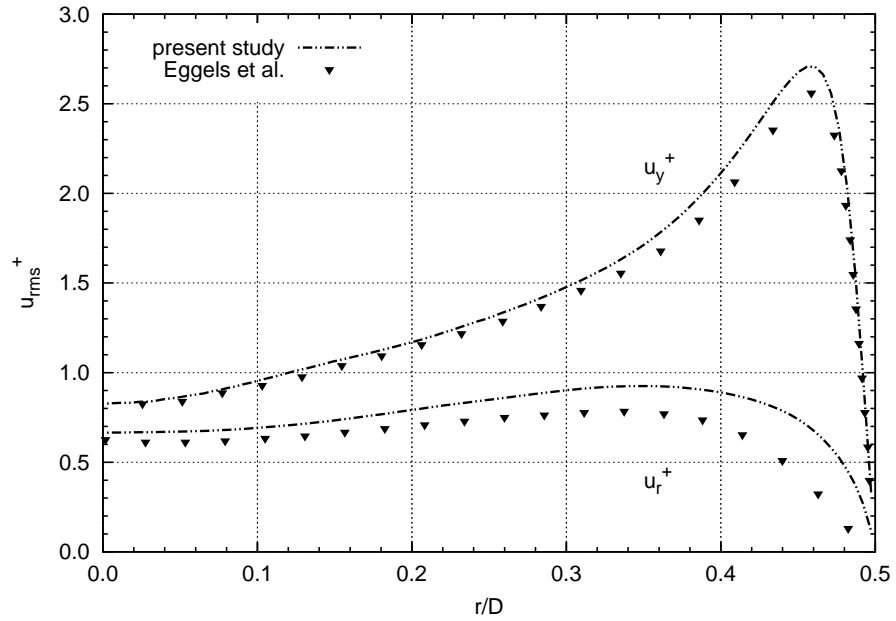


Figure 3: Root-mean-square velocities in wall coordinates, u_{rms}^+ , as function of the distance from the centerline, r/D .

4.2 Turbulent flow over a spherical bubble

The numerical simulation of the flow over a spherical bubble is started, at dimensionless time $t^* = 2u_{bl}t/d = 0$, with the velocity field obtained from the simulation of the turbulent pipe flow at $Re = 5300$. This initial velocity field evolves during a transient period in order to reach the new Reynolds number of the pipe flow, $Re = 6000$, while at the same time generates a wake behind the bubble and a vortical flow inside of it. Hence, the simulation is advanced in time until statistically stationary flow conditions are achieved at $t^* = 20$, then, the collection of average data is initialized until $t^* = 50$. Additionally to averaging in time, the statistical data is also averaged in the rotational direction.

As an example, the instantaneous flow at $t^* = 40$ is shown in Fig. 4. The figure shows the turbulent flow in the pipe, while at the same time shows a close view of the flow over the spherical bubble in a superimposed image. It can be observed that the presence of the bubble generates a wake, similarly to the case of a solid sphere, however, the fact that the fluid slips through the surface of the bubble instead of stopping, produces, due to viscosity, a transfer of momentum from the fluid surrounding the bubble to the fluid inside of it. This continuous transfer of momentum generates a turbulent vortical flow inside the bubble, as it can be seen in Fig. 5, making the instantaneous y -velocity at the center of the bubble oscillate approximately as -1.8 ± 0.08 .

The time- and rotational-averaged axial velocity on the y -axis of the pipe and its profiles on the radial direction at different positions near the bubble are plotted in Fig. 6 and Fig. 7, respectively. The detailed inspection of Fig. 6 reveals three important aspects of the flow configuration around the bubble. First, similarly to a case with a solid sphere, the axial velocity on the upstream part of the bubble corresponds to the one imposed by the turbulent behaviour of the flow inside the pipe, $u_y/u_{bl} = 0.62$, while close to the bubble, the velocity is reduced to zero parabolically when reaching the stagnation point, $y/d = -0.5$. Second, as visualized in Fig. 5, the axial velocity inside the bubble is characterized by the presence of a toroidal vortex of the size of the bubble. Hence, two short recirculation zones are generated at the extremes of the bubble's diameter, and in between, the axial velocity evolves by changing its sign down to a value of $u_y/u_{bl} = -1.04$. Notice that this minimum value is not found exactly at the center of the bubble. In particular, it is found at $y/d = -0.06$, thus, the maximum velocity (in absolute value) is



Figure 4: Velocity magnitude of the flow around the bubble in the turbulent pipe flow at $t^* = 40$.

pushed to the upstream part of the center of the bubble. Third, similarly once again to a case of a solid sphere, on the downstream part of the bubble a wake is generated. It starts with a zero axial velocity at $y/d = 0.5$, is followed by a recirculation zone of length $L_r/d = 0.5$ and is finalized by a smooth transition to the mean axial velocity determined by the turbulent flow configuration of the pipe.

The description of the flow over the bubble is complemented by studying the averaged axial velocity profiles on the radial direction. Hence, Fig. 7 shows this quantity at positions $y/d = -1.0$, $y/d = -0.5$, $y/d = 0.0$, $y/d = 0.5$ and $y/d = 1.0$. In particular, the analysis of the figure is performed by describing the evolution of the axial velocity in three zones: (A) $r/d = 0.0 - 0.1$, (B) $r/d = 0.1 - 0.6$ and (C) $r/d = 0.6 - 0.8$. First, zone A is characterized by a constant value of the axial velocity at each position: $u_y/u_{bl} = 0.62$ at $y/d = -1.0$ (axial mean velocity in the pipe), $u_y/u_{bl} = 0.0$ at $y/d = -0.5, 0.5, 1.0$ (recirculation zones) and $u_y/u_{bl} = -1.0$ at $y/d = 0.0$ (axial velocity on the center of the bubble). Second, zone B corresponds to the vicinity of the bubble's surface. Notice how, at $r/d = 0.5$, the flow is accelerated from $u_y/u_{bl} = 0.62$ at $y/d = -0.5$ to $u_y/u_{bl} = 1.0$ at $y/d = 0.0$, and then, is decelerated again to $u_y/u_{bl} = 0.62$ at $y/d = 0.5$. Thus, the maximum axial velocity on the surface of the bubble corresponds (in absolute value) to the axial velocity on the center of the bubble, u_{bl} . Furthermore, according to the slip condition on the bubble's surface, no boundary layer is generated and, due to viscosity, momentum is transferred from the fluid surrounding the bubble to the fluid inside of it. This makes the lighter fluid inside the bubble reach a higher velocity in the vicinity of the bubble's surface, as it can be seen in the $y/d = 0.0$ profile between $r/d = 0.4$ and $r/d = 0.5$. Finally, zone C corresponds to the undisturbed flow along the pipe equal to the mean axial velocity $u_y/u_{bl} = 0.62$.

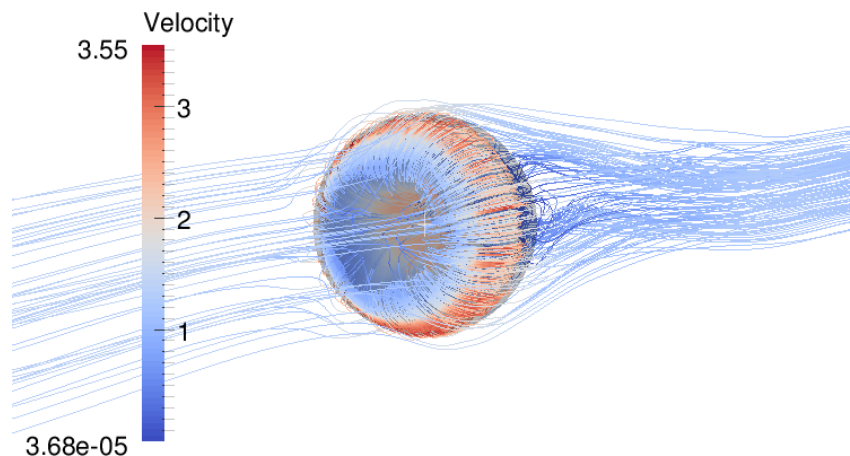


Figure 5: Streamlines of the instantaneous velocity of the flow over the bubble at $t^* = 40$.

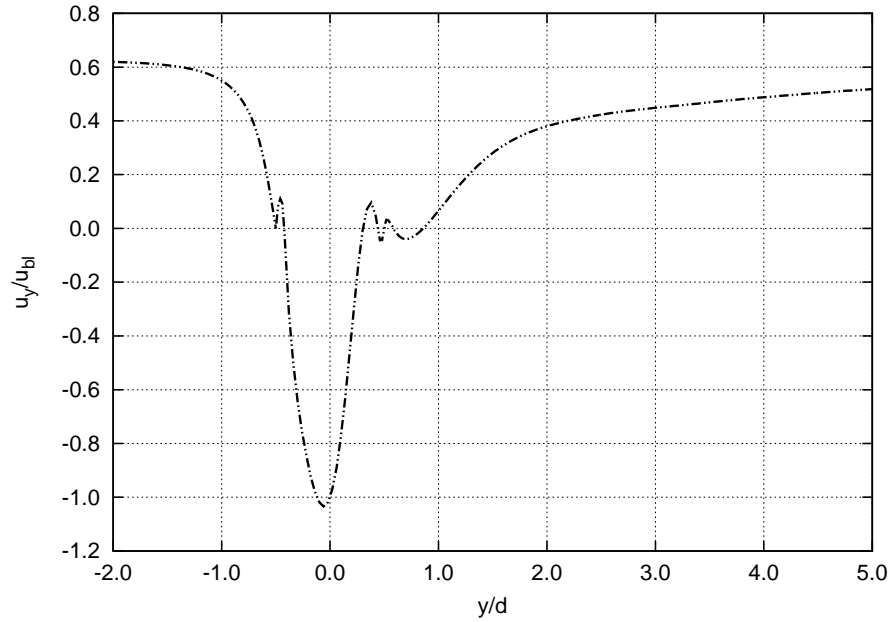


Figure 6: Axial mean velocity, u_y , normalized by the bubble velocity, u_{bl} , on the y -axis of the pipe as function of y distance from the center of the bubble normalized by the diameter of the bubble, d .

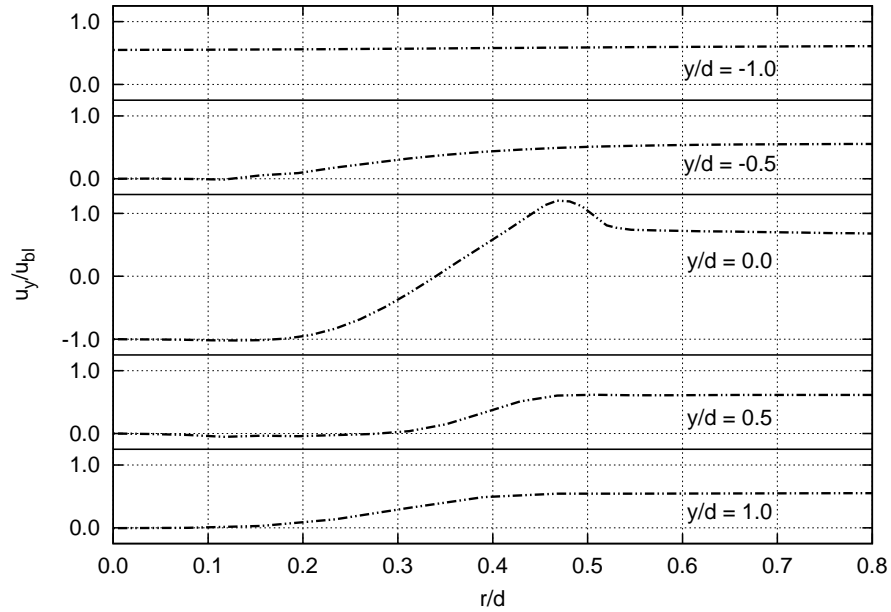


Figure 7: Profiles of the axial mean velocity, u_y , normalized by the bubble velocity, u_{bl} , as function of the distance from the centerline, r/d , at $y/d = -1.0$, $y/d = -0.5$, $y/d = 0.0$, $y/d = 0.5$ and $y/d = 1.0$.

5 CONCLUSIONS

A first attempt to simulate the flow over a spherical bubble, $Re_{bl} = 500$, in a turbulent pipe flow, $Re = 6000$, has been carried out by means of DNS. The numerical model utilized captures interfaces with a VOF method and discretizes the mass and momentum equations by means of a collocated scheme. In particular, the discretization utilized conserves mass and momentum exactly, while minimizes the error in the conservation of kinetic energy by using a symmetry-preserving convection scheme and scaling the error intrinsic to the collocated schemes as $\mathcal{O}(\Delta h^2, \Delta t^m)$. The results have been computed on a mesh of 5.4M cells, resulting from rotating 128 times a 2-D grid discretized by means of 128 and 330 points in the radial and axial directions, respectively. Moreover, the data have been time- and rotational-averaged in order to study the turbulent steady state behaviour of the flow.

Prior to simulating the flow over the spherical bubble, the solution of the turbulent pipe flow at $Re = 5300$ without the bubble has been solved. This test has checked the numerical model without interfaces and, simultaneously, has generated a fully developed turbulent flow useful to start the simulation of the bubble. Next, the simulation of the flow over the bubble has concluded that its presence generates a wake, similarly to the case of a solid sphere, however, it differs in the fact that the fluid slips through the surface of the bubble instead of stopping, thus, no boundary layer is created and, due to viscosity, a transfer of momentum from the fluid surrounding the bubble to the fluid inside of it is produced. This transfer of momentum generates a turbulent toroidal vortex inside the bubble. In consequence, two short recirculation zones are found at the extremes of the bubble's diameter, while in between, the axial velocity inverts its sign. Furthermore, it has been found that the flow on the surface of the bubble is accelerated to a value equal (in absolute value) to the axial velocity on the center of the bubble, and then is decelerated back to the mean axial velocity of the pipe.

This has been a first study of the flow over a spherical bubble in a turbulent pipe flow, thus, still some studies need to be performed in order to fully understand the physics of this case. For instance, the integration in time of the instantaneous data should be performed on larger periods, grid resolution studies and the analysis of second-order statistics are needed, also, a study of the power spectra at different points would be very useful, since it would provide the frequency of the vortex-shedding mechanism of this problem.

ACKNOWLEDGEMENTS

This work has been financially supported by the Ministerio de Economía y Competitividad, Secretaría de Estado de Investigación, Desarrollo e Innovación, Spain (ENE-2010-17801 and ENE-2011-28699), a FPU Grant by the Ministerio de Educación, Cultura y Deporte, Spain (AP-2008-03843) and by Termo Fluids S.L.

REFERENCES

- [1] J. Magnaudet and I. Eames. The Motion of High-Reynolds-Number Bubbles in Inhomogeneous Flows. *Annu. Rev. Fluid Mech.*, Vol. **32**, 659–708, 2000.
- [2] J. Magnaudet, M. Rivero and J. Fabre. Accelerated Flows Past a Rigid Sphere or a Spherical Bubble. Part 1. Steady Straining Flow. *J. Fluid Mech.*, Vol. **284**, 97–135, 1995.
- [3] D. Legendre and J. Magnaudet. The Lift Force on a Spherical Bubble in a Viscous Linear Shear Flow. *J. Fluid Mech.*, Vol. **368**, 81–126, 1998.
- [4] J. Magnaudet and D. Legendre. The Viscous Drag Force on a Spherical Bubble with a Time-Dependent Radius. *Phys. Fluids*, Vol. **10**, 550–555, 1998.
- [5] J. Magnaudet and D. Legendre. Some Aspects of the Lift Force on a Spherical Bubble. *Appl. Sci. Res.*, Vol. **58**, 41–61, 1998.
- [6] A. Merle, D. Legendre and J. Magnaudet. Forces on a High-Reynolds-Number Spherical Bubble in a Turbulent Flow. *J. Fluid Mech.*, Vol. **532**, 53–62, 2005.
- [7] C. W. Hirt and B. D. Nichols. Volume of fluid (VOF) Method for the Dynamics of Free Boundaries. *J. Comput. Phys.*, Vol. **39**, 201–225, 1981.
- [8] S. Osher and J. Sethian. Fronts Propagating with Curvature Dependent Speed: Algorithms Based on Hamilton-Jacobi Formulations. *J. Comput. Phys.*, Vol. **79**, 12–49, 1988.
- [9] L. Jofre, O. Lehmkuhl, J. Castro and A. Oliva. A 3-D Volume-of-Fluid Advection Method Based on Cell-Vertex Velocities for Unstructured Meshes. *Comput. Fluids*, Vol. **94**, 14–29, 2014.
- [10] L. Jofre, O. Lehmkuhl, J. Ventosa, F. X. Trias and A. Oliva. Conservation Properties of Unstructured Finite-Volume Mesh Schemes for the Navier-Stokes Equations. *Numer. Heat Tr. B-Fund.*, Vol. **65**, 53–79, 2014.
- [11] R. W. C. P. Verstappen and A. E. P. Veldman. Symmetry-Preserving Discretization of Turbulent Flow. *J. Comput. Phys.*, Vol. **187**, 343–368, 2003.
- [12] J. G. M. Eggels, F. Unger, M. H. Weiss, J. Westerweel, R. J. Adrian, R. Friedrich and F. T. M. Nieuwstadt. Fully Developed Turbulent Pipe Flow: a Comparison between Direct Numerical Simulation and Experiment. *J. Fluid Mech.*, Vol. **268**, 175–209, 1994.
- [13] D. W. Moore. The Boundary Layer on a Spherical Gas Bubble. *J. Fluid Mech.*, Vol. **16**, 161–176, 1963.
- [14] R. Borrell, O. Lehmkuhl, F. X. Trias and A. Oliva. Parallel Direct Poisson Solver for Discretizations with one Fourier Diagonalizable Direction. *J. Comput. Phys.*, Vol. **230**, 4723–4741, 2011.